Effect of Proton Pump Inhibitor Pretreatment on Resistance of Solid Tumors to Cytotoxic Drugs

Francesca Luciani, Massimo Spada, Angelo De Milito, Agnese Molinari, Licia Rivoltini, Annalisa Montinaro, Manuela Marra, Luana Lugini, Mariantonia Logozzi, Francesco Lozupone, Cristina Federici, Elisabetta Iessi, Giorgio Parmiani, Giuseppe Arancia, Filippo Belardelli, Stefano Fais

Background: **Resistance to antitumor agents is a major cause of treatment failure in patients with cancer. Some mechanisms of tumor resistance to cytotoxic drugs may involve increased acidification of extracellular compartments. We investigated whether proton pump inhibitors (PPIs), currently used in the anti-acid treatment of peptic disease, could inhibit the acidification of the tumor microenvironment and increase the sensitivity of tumor cells to cytotoxic agents.** ***Methods:*** **We pretreated cell lines derived from human melanomas, adenocarcinomas, and lymphomas with the PPIs omeprazole, esomeprazole, or pantoprazole and tested their response to cytotoxic drugs in cell death assays. We also evaluated extracellular and intracellular pH and vacuolar-H^+-ATPase (V-H^+-ATPase) expression, distribution, and activity in PPI-pretreated cells by using western blot analyses, immunocytochemistry, laser scanning confocal analysis, and bioluminescence assays. Finally, we evaluated human melanoma growth and cisplatin sensitivity with or without omeprazole pretreatment in xenografted SCID/SCID mice.** ***Results:*** **PPI pretreatment sensitized tumor cell lines to the effects of cisplatin, 5-fluorouracil, and vinblastine, with an IC_{50} value reduction up to 2 logs. PPI pretreatment was associated with the inhibition of V-H^+-ATPase activity and increases in both extracellular pH and the pH of lysosomal organelles. PPI pretreatment induced a marked increase in the cytoplasmic retention of the cytotoxic drugs, with clear targeting to the nucleus in the case of doxorubicin. In *in vivo* experiments, oral pretreatment with omeprazole was able to induce sensitivity of human solid tumors to cisplatin.** ***Conclusion:*** **Our results open new possibilities for the treatment of drug-resistant tumors through combination strategies based on the use of well-tolerated pH modulators such as PPIs. [J Natl Cancer Inst 2004;96:1702–13]**

Resistance to cytotoxic agents is a major problem in treating cancer *(1).* The mechanisms underlying this phenomenon appear to take advantage of functions involved in the control of cell homeostasis. The overexpression of P-glycoprotein, a plasma membrane drug efflux transporter that belongs to the ATP binding-cassette transporter family, represents one major mechanism by which tumors become multidrug resistant *(1).* Another mechanism of resistance may be alteration of the tumor microenvironment via changes in the pH gradient between the extracellular environment and the cell cytoplasm and/or in the pH gradient between the cell cytoplasm and lysosomal compartments *(2,3).* The extracellular (i.e., interstitial) pH of solid tumors is substantially more acidic than that of normal tissues *(4,5),* and the acidic pH of the tumor microenvironment may impair the uptake of weakly basic chemotherapeutic drugs *(6,7).* Indeed, in animal models, bicarbonate-induced extracellular alkalinization leads to substantial improvement in the therapeutic effectiveness of antitumor drugs *(2,8).*

The pH gradient between the cytoplasm and intracellular organelles may be also involved in resistance to antitumor drugs. The suggested mechanisms are drug sequestration and neutralization in acidic organelles or in the acidic extracellular environment *(6,7,9–12).* Increased turnover of acidic vesicles may represent an additional important feature of the mechanism for chemoresistance, both in cells overexpressing multidrug efflux transporters such as P-glycoprotein *(13–15)* and in cells that do not express these efflux transporters *(16).* The involvement of acidic vesicles in resistance to cytotoxic drugs includes both an increased acidification of lysosomal-type vesicles, leading to sequestration of drugs in acidic organelles, and drug extrusion from the cell through a secretory pathway *(6,7,9–14,17).*

Agents that disrupt the pH gradient in tumors may be an option for reversing multidrug resistance. For example, the induction of pH gradient modifications through lysosomotropic

Affiliations of authors: Departments of Infectious, Parasitic and Immune-Mediated Diseases (F. Luciani), Cell Biology and Neuroscience (MS, FB), Drug Research and Evaluation (ADM, A. Montinaro, LL, ML, F. Lozupone, CF, EI, SF), and Health and Technology (A. Molinari, MM, GA), Istituto Superiore di Sanità, Rome, Italy; Unit of Immunotherapy of Human Tumors (LR, GP), Istituto Nazionale dei Tumori, Milan, Italy.

Correspondence to: Stefano Fais, MD, PhD, Department of Drug Research and Evaluation, Pharmacogenetic, Drug Resistance and Experimental Therapeutic Section, Istituto Superiore di Sanità 00161, Rome, Italy (e-mail: fais@iss.it).

See "Notes" following "References."

DOI: 10.1093/jnci/djh305

agents may reverse anthracycline resistance in multidrug-resistant cells with an expanded acidic lysosomal compartment *(18).* Another approach may be to inhibit the function of the pumps that establish the pH gradient. Vacuolar-H+-ATPases (V-H^+-ATPases) represent a major mechanism in the regulation of cellular pH *(19).* V-H^+-ATPases pump protons across the plasma membrane and across the membranes of a wide array of intracellular compartments *(19).* Some human tumor cells, particularly those selected for multidrug resistance, exhibit enhanced V-H^+-ATPase activity *(20–25).* These data suggest that the enhanced V-H^+-ATPase activity increases the acidity of intracellular vesicles, allowing drug sequestration and consequently the development of multidrug resistance. Some molecules that inhibit V-H^+-ATPases and may revese tumor resistance to cytotoxic drugs have been identified *(5,6,18,26).* However, their toxicity and poor results in preclinical testing have limited their development as therapeutic agents.

A class of H^+-ATPase inhibitors called proton pump inhibitors (PPIs) has emerged as the drug class of choice for treating patients with peptic disease, including gastroesophageal reflux disease and duodenal or gastric ulcers. These anti-acid drugs inhibit gastric acid secretion by targeting the gastric acid pump *(26–30).* Their effects at the cellular level are mediated by direct inhibition of V-H^+-ATPase *(31–33).* PPIs, which include omeprazole, esomeprazole, lansoprazole, pantoprazole, and rabeprazole, are substituted 2-pyridyl-methylsulfinyl benzimidazoles that share a similar core structure *(30).* These agents are protonatable weak bases with pK_a (negative logarithm of the acid ionization constant) values of approximately 4, with the exception of rabeprazole, which has a pK_a of 5. Therefore, PPIs accumulate selectively in acidic spaces with a pH of less than 4. In such acidic environments, protonation of the pyridine and benzimidazole nitrogens results in formation of a tetracyclic sulfenamide, which is the active form of the drug *(30).*

The aim of our work was to determine whether PPIs can restore drug sensitivity to drug-resistant cells by inhibiting the increased acidification of both the intracellular compartments and the extracellular spaces in the tumor, possibly through a V-H^+-ATPase–mediated mechanism. We examined this hypothesis both *in vitro,* using human tumor cell lines displaying intrinsic or acquired resistance to antitumor drugs, and *in vivo,* in an animal model represented by CB.17 SCID/SCID mice engrafted with human tumor cells.

Materials and Methods

Drugs

Omeprazole and esomeprazole (AstraZeneca, Mölndal, Sweden) and pantoprazole (Byk Gulden, Konstanz, Germany) sodium salts were resuspended in normal saline (0.85%) at a concentration of 1 mg/mL immediately before use. Cisplatin (Aventis, Schiltigheim, Germany) was resuspended in phosphate-buffered saline (PBS) at a stock concentration of 1 mg/mL and stored at –20 °C. This stock solution was thawed immediately before use and not refrozen. 5-Fluorouracil (5-FU; Teva Pharma, Haarlem, The Netherlands) was supplied in solution at a concentration of 50 mg/mL and was stored at room temperature, as indicated by the supplier. Vinblastine sulfate (Eli Lilly, Paris, France) was suspended in ethanol:distilled water (1:1000) at a concentration of 0.1 mg/mL; this stock solution was stored at 4 °C and used within 3 days. Vinblastine-bodipy was obtained from Molecular Probes (Eugene, OR) and stored at –20 °C as stock solution at 0.1 mg/mL in dimethyl sulfoxide (DMSO).

Tumor Cells

Human drug-resistant tumor cell lines (from 22 melanomas, two colon adenocarcinomas, two breast cancers, and two ovarian carcinomas) were supplied by Istituto Nazionale per lo Studio e la Cura dei Tumori, Milan, Italy, and were obtained from primary lesions. HeLa and CEM-CCRF T-lymphoblastoid cells (referred to as CEM cells) were obtained from American Type Culture Collection (Manassas, VA). The CEM-VBL100 cell line, a multidrug-resistant P-glycoprotein–overexpressing variant of CEM cells, was selected in our laboratory. These cells were produced by exposing parental CEM cells to increasing sublethal concentrations of vinblastine up to 100 ng/mL *(34).* All cells were cultured in RPMI-1640 medium supplemented with 10% fetal calf serum (FCS) and antibiotics, in humidified 5% CO_2.

Dose–Response Curves

Tumor cells growing in suspension (CEM and CEM-VBL100 cells) were plated at 1.5×10^5 cells per milliliter in 24-well plates at one milliliter per well. Tumor cells growing in adherence (melanoma and colon, breast, and ovarian cancer cell lines) were plated at 3×10^4 cells per well in 24-well plates. After 24 hours, each cell line was treated with three to five logarithmic dilutions of each of the drugs. Each drug was tested on each cell type in triplicate. In combined treatment experiments, cells were pretreated for 24 hours with the PPI and were then treated for an additional 24 hours with the antitumor drug.

Cytotoxicity Assays

Trypan blue exclusion method. After treatment, cells growing in suspension were collected, centrifuged 5 minutes at 500*g,* and resuspended in 30 μL of PBS. Cells growing in adherence were collected by pooling cells from the medium (i.e., dead cells) and adherent (live) cells obtained by trypsinization. Cells were then centrifuged (10 minutes at 500*g*) and resuspended in PBS (50–100 μL). An aliquot of each cell line suspension was diluted 1:1 (vol/vol) with 0.4% trypan blue. After 5 minutes, cells were loaded on a hemocytometer, and both live (unstained) and dead (blue-stained) cells were counted under a light microscope. The percentage of dead cells was then determined. Each treatment condition was tested at least in triplicate, and the mean value (% dead cells) was determined.

LIVE/DEAD Viability/Cytotoxicity assay. The LIVE/DEAD Viability/Cytotoxicity Assay (Molecular Probes, Eugene, OR) is a two-color fluorescence cell viability assay that is based on the simultaneous determination of live and dead cells with two probes (i.e., calcein AM and ethidium homodimer 1, respectively) that measure two recognized parameters of cell viability (i.e., intracellular esterase activity and plasma membrane integrity, respectively). The optimal dye concentrations for the cell types used in this study were determined according to manufacturer's instructions. After treatment, cells were collected, centrifuged, and resuspended in PBS as described above, treated with calcein AM and ethidium homodimer 1 at the final concentrations of 0.1 μ*M* and 1 μ*M,* respectively, and left at room temperature for 30 minutes. The cells were then washed in PBS,

and the samples were analyzed with a FACScan cytometer (Becton Dickinson, Franklin Lakes, NJ). At least 20 000 events were acquired with at least three replicates for each treatment condition.

Determination of Cell Cycle

Cell cycle distribution was analyzed as described *(35)*. Briefly, 0.2×10^6 cells were washed in PBS and incubated overnight in 400 μL of ice-cold 70% ethanol. After two washes in PBS, the cells were incubated for 30 minutes at 37 °C in PBS containing 100 μg/mL DNAse-free RNAse and 40 μg/mL propidium iodide. The samples were then acquired with a FACScan cytofluorimeter that collected the fluorescence signal in FL2 channel on a linear scale and analyzed using CellQuest and ModFIT software (Becton Dickinson).

Laser Scanning Confocal Microscopy Analysis

For laser scanning confocal microscopy (LSCM) analysis of drug uptake and efflux, cells (3×10^4 cells per well) were plated on glass coverslips in 24-well plates. After the cells had adhered, the medium was replaced with fresh medium (1 mL) containing a PPI at the appropriate concentration. After 24 hours, this medium was removed and fresh medium (1 mL) supplemented with 0.1 μg/mL vinblastine-bodipy or 5 μ*M* doxorubicin was added to cells. After 6 hours (uptake phase), drug-containing medium was removed and the cells were incubated in drug-free medium for up to 36 hours (efflux phase). Cells were observed with a Leica TCS SP2 spectral confocal microscope, as previously described *(36)*. Doxorubicin fluorescence was excited with a 488-nm argon laser, and emission lines were collected after passage through a DD 488/543 filter in a spectral window ranging from 515 to 600 nm. Vinblastine-bodipy fluorescence was excited at the 488-nm argon laser line, and emission lines were collected after passage through a DD 488/543 filter in a spectral window ranging from 515 to 565 nm. Pixel intensity was analyzed with the Quantify Leica TCS SP2 program. Mean pixel intensities, evaluated on 255 gray levels, were calculated by analyzing a total cell area of 25 000 μm^2 for each sample. The calculation was performed on images representing orthogonal maximum projections of 20 optical sections (0.5 μm thick) acquired with the following acquisition parameters: 63.0/1.4 NA objective; image size: 1024×1024 pixels; pinhole size: 1 Airy.

Sodium Dodecyl Sulfate–Polyacrylamide Gel Electrophoresis and Western Blotting

Sodium dodecyl sulfate–polyacrylamide gel electrophoresis and western blot analysis of V-H^+-ATPase was performed as previously described *(35)*. Briefly, melanoma cells were lysed in Akt buffer (150 m*M* NaCl, 20 m*M* Tris–HCl [pH 7.4], 1% NP40, 10% glycerol) supplemented with protease and phosphatase inhibitors (aprotinin, leupeptin, phenylmethylsulfonyl fluoride, sodium orthovanadate) incubated for 15 minutes on ice, and centrifuged at 13 000*g* for 15 minutes to remove nuclei and cell debris. The protein concentration of the extracts was determined by the Bio-Rad Protein Assay (Bio-Rad, Hercules, CA), following the manufacturer's instructions. Fifty micrograms of each cell extract was separated on 10% gels and electroblotted to a nitrocellulose membrane. Nonspecific binding was blocked by incubating the membrane in 1× PBS with 5% nonfat dry milk. Blots were then incubated with a polyclonal goat anti-human antibody to V-H^+-ATPase subunit C (Santa Cruz Biotechnology, Santa Cruz, CA) and a monoclonal mouse anti-human antibody to actin (Chemicon, Temecula, CA) as a control for protein loading. Antibody binding was detected by incubating the blot with a horseradish peroxidase–conjugated rabbit anti-goat antibody (Jackson Immunoresearch, West Grove, PA) and then with a horseradish peroxidase–conjugated sheep anti-mouse antibody (Amersham, Piscataway, NJ), respectively. Antibody staining was visualized by enhanced chemiluminescence (Pierce, Rockford, IL).

Determination of Intracellular ATP Concentration

We measured the amount of available intracellular ATP in melanoma cell lines as an indirect parameter *(37)* of the activity of V-H^+-ATPases. We used a commercially available ATP Determination Kit (Molecular Probes) that is based on luciferase activity. Cells were cultured for 24 hours in 24-well plates at a density of 0.05×10^6 cells per well in the presence of a PPI (1 μg/mL). ATP determination was performed by using the ATP Determination Kit, as reported elsewhere *(37)*. Briefly, 10 000 cells were collected, washed in PBS, resuspended in 100 μL of distilled water, and boiled for 5 minutes. Ten μL of each sample (1000 cells) or 10 μL of each dilution point of ATP standard solution (0–1000 n*M*) was added to 90 μL of reaction solution in the wells of 96-well plates. After 5 minutes, plates were analyzed with a luminometer (Wallac 1420 VICTOR; Wallac, Boston, MA). The amount of intracellular ATP was determined by plotting the light output values of each sample against those of the ATP standard solutions. All experiments were run in duplicate, and mean values were calculated.

Determination of Extracellular pH

MelM1, MelM6, MelM9, and MelP6 cells were incubated in a medium (pHmed) made up of normal saline (80%), RPMI-1640 (10%), and FCS (10%). This composition minimized the buffering activity of phosphate and bicarbonate in the medium but still contained sufficient nutrients and growth factors to support cell growth (data not shown). Untreated cells were harvested, washed twice in pHmed, and then incubated at 2×10^6 cells per milliliter in pHmed for 3 hours at 37 °C. The cells were then collected by centrifugation (10 minutes at 500*g*), and the supernatant was harvested for pH measurements. pH was determined by reading each sample at 32 °C, in triplicate, using a Titroprocessor 726 pH meter (Metrohm, Herisau, Switzerland) equipped with a glass microelectrode (LongLife; Metrohm). Data are presented as means with 95% confidence intervals (CIs).

Staining of Acidic Vesicles With a pH Indicator

The LysoSensor Green DND-189 probe (Molecular Probes), which accumulates in acidic vesicles and exhibits a pH-dependent increase in fluorescence intensity on acidification, was used according to the manufacturer's indications to measure the effects of omeprazole treatment on acidic vesicles. Briefly, 5×10^5 MelM6 cells were collected after 24 hours of omeprazole treatment (1 μg/mL) and washed twice in PBS. Cells were then incubated for 5 minutes at 37 °C with 500 μL of prewarmed PBS containing 1 μ*M* LysoSensor probe and analyzed by flow cytometry collecting FL1 fluorescence. Untreated and unstained cells were used to set the background fluorescence. The exper-

iment was repeated twice. For analysis of the localization of LysoSensor-positive vesicles, cells were incubated for 1 hour at 37 °C with prewarmed PBS containing the LysoSensor probe and analyzed by LSCM, as described above.

Histology and Immunocytochemistry

Human tumors were fixed in 10% formalin and embedded in paraffin. Four-micrometer sections were cut, stained with hematoxylin and eosin, and examined under the microscope. MelM6 cells (3×10^4 cells per chamber) were attached to sterile glass chamber slides (LabTek, Naperville, IL) by overnight incubation in 150 μL of RPMI-1640 per well in a humidified 5% CO_2 atmosphere. Cells were then fixed in cold 70% methanol (10 minutes at 4 °C) and stained with polyclonal goat anti-human V-H^+-ATPase antibodies (Santa Cruz, CA) using the alkaline phosphatase anti–alkaline phosphatase (APAAP) method (Dako, Glostrup, Denmark), as described *(38).*

In Vivo Tumor Growth Analyses

Female CB.17 SCID/SCID mice aged 4–5 weeks (Harlan; Correzzana, Milan, Italy) were kept under specific pathogen-free conditions and fed *ad libitum.* The mice *(39)* were housed in micro-isolator cages, and all food, water, and bedding were autoclaved prior to use. Each mouse was injected subcutaneously in the right flank with 3×10^6 human melanoma or colon adenocarcinoma cells derived from metastatic lesions that had been resuspended in 0.2 mL of RPMI-1640 containing 10% FCS. Once tumors became evident (at least 0.10×0.10 cm, approximately 10 days after the tumor cell injection), PPI (omeprazole, esomeprazole, or pantoprazole sodium salts resuspended in normal saline at a concentration of 15 mg/mL immediately before use) was orally administered by gavage *(40)* at a dose of 75 mg/kg. Cisplatin was administered by intraperitoneal injection at a dose of 5 mg/kg *(41)* simultaneously with PPI oral treatment, 24 hours after PPI treatment, or in mice that did not receive any PPI treatment. Tumor dimensions were measured three times per week with calipers. Tumor weight was estimated according to Geran et al. *(42)* using the following formula: tumor weight (mg) = length (mm) $\times$ width^2 (mm)/2.

At least 10 mice were used for each treatment group. Data are expressed as the mean value of tumor weight with 95% confidence intervals. Mice were monitored for the duration of the *in vivo* experiments for body weight, hair ruffling, and the presence of diarrhea. All mice were killed at the end of the experiments, within months after the injection of the human tumor cells (following the guidelines of the Istituto Superiore di Sanità).

Statistical Analysis

Data from the LIVE/DEAD Viability/Toxicity assay were recorded and statistically analyzed on a Macintosh computer with CellQuest software. Fluorescence intensity (expressed as median values) was calculated after logarithmically amplified signals were converted to a linear scale. Statistical significance of the difference in mean fluorescence intensity between PPI pretreatred and untreated cells was calculated with the parametric Kolmogorov–Smirnov test. Statistical analysis of data from the trypan blue exclusion test was performed with the Student's *t* test. Only *P* values of less than .01 were considered statistically significant. One-way analysis of variance with a pairwise multiple comparison procedure (Tukey test) was used to analyze the statistical significance of tumor weight differences between the treatment groups in the *in vivo* experiments carried out in tumor-engrafted SCID mice.

Results

Effect of PPI Pretreatment on Drug-Resistant Human Tumor Cells

We first examined whether the PPIs omeprazole, esomeprazole, or pantoprazole could reverse the intrinsic resistance of human tumor cells to cytotoxic drugs. In designing the experiments, we considered that cisplatin can enhance the activity of proton pumps *(25),* that PPIs must be protonated in an acidic environment to function as PPIs *(30),* and that PPIs and antitumor drugs, such as cisplatin, 5-FU, and vinca alkaloids, are all weakly basic molecules that would thus compete for sequestration by protonation in acidic microenvironments. However, an important difference between PPIs and the anticancer drugs is that protonation activates PPIs but neutralizes (i.e., inactivates) the weakly basic antitumor drugs. Moreover, tumor cells were cultured in buffered media, which maintains the pH of tumor cell cultures approximately at neutrality. Therefore, under culture conditions, the only possible place where the acidity of the tumor cell microenvironment could reach levels more suitable for PPI protonation (i.e., a pH of <4) is in close proximity to the plasma membrane of the tumor cells. Thus, we hypothesized that the best approach to test the effect of PPIs in inhibiting intrinsic resistance to antitumor drugs would be to avoid possible competition between PPIs and the tumor drugs at the tumor cell level.

We therefore performed a first set of experiments to compare the effect of pretreating tumor cells with a PPI and then treating them with a cytotoxic drug with the effect of treating tumor cells with a PPI and an antitumor drug simultaneously. In these experiments, human tumor cell lines of different histologies (22 melanoma, two colon adenocarcinoma, two breast cancer, and two ovarian carcinoma), all of which had been determined by a trypan blue exclusion assay to be resistant to the cytotoxic effects of cisplatin (Table 1), were treated with cisplatin after a 24-hour pretreatment with omeprazole. The 24-hour PPI pretreatment was chosen on the basis of preliminary experiments showing more reproducible results than those obtained with shorter (6 or 12 hours) or longer (36 hours) PPI pretreatments (data not shown). We used two different approaches to evaluate the cytotoxic effects of cisplatin (% of dead cells after 24 hours of treatment with the drug) that provided fully comparable and reproducible results. Dose–response curves for cisplatin were obtained by pretreating cells for 24 hours with omeprazole or with saline and then treating them with one of three logarithmic dilutions of cisplatin. The results of repeated experiments with three melanoma lines (Fig. 1, A–C) indicated that pretreatment with omeprazole induced susceptibility of melanoma cells to the cytotoxic effect of cisplatin. Similar results were obtained with other tumor cell lines and other PPIs (Table 1). Figure 1, D, shows the results of repeated experiments in which a melanoma cell line was pretreated with esomeprazole and then with cisplatin, providing data similar to those obtained with omeprazole.

Table 1. IC_{50} data for cisplatin (CPL), 5-fluorouracil (5-FU), and vinblastine (VBL) on 28 human cancer cell lines, with no pretreatment or after 24-hour pretreatment with omeprazole or esomeprazole*

	Pretreatment								
	None			Omeprazole			Esomeprazole		
Cell line	CPL (μM)	5-FU (μg/mL)	VBL (ng/mL)	CPL (μM)	5-FU (μg/mL)	VBL (ng/mL)	CPL (μM)	5-FU (μg/mL)	VBL (ng/mL)
Mel P1	>500	627.3	>1000	69.3	9.5	50.0	110.2	11.1	35.5
Mel P2	>500	756.0	n.d.	109.6	10.2	n.d.	86.8	17.6	n.d.
Mel P3	445.0	>1000	n.d.	59.7	31.5	n.d.	26.6	15.5	n.d.
Mel P4	390.0	850.5	n.d.	1.5	1.3	n.d.	2.6	0.8	n.d.
Mel P5	>500	>1000	n.d.	10.9	23.7	n.d.	9.5	19.2	n.d.
Mel P6	>500	>1000	>1000	62.5	110.7	42.6	100.5	5.7	12.5
Mel P7	250.6	799.5	n.d.	9.8	0.6	n.d.	12.6	1.1	n.d.
Mel P8	406.0	>1000	n.d.	49.7	33.2	n.d.	31.3	35.4	n.d.
Mel M1	367.0	>1000	>1000	28.6	15.1	31.6	24.9	12.3	34.4
Mel M3	>500	660.3	n.d.	41.6	2.8	n.d.	38.6	5.2	n.d.
Mel M4	>500	>1000	n.d.	52.3	26.3	n.d.	48.9	42.0	n.d.
Mel M5	>500	>1000	n.d.	89.4	47.0	n.d.	105.3	15.5	n.d.
Mel M6	399.5	>1000	>1000	0.1	0.1	15.7	0.7	0.5	9.9
Mel M7	275.0	>1000	n.d.	15.5	66.3	n.d.	18.7	52.5	n.d.
Mel M8	>500	>1000	n.d.	17.3	3.9	n.d.	11.5	5.2	n.d.
Mel M9	269.0	585.6	>1000	0.6	12.6	16.5	0.8	8.9	17.9
Mel M10	>500	>1000	n.d.	100.6	52.0	n.d.	65.2	35.9	n.d.
Mel M11	>500	>1000	n.d.	99.7	39.0	n.d.	75.8	22.3	n.d.
Mel M12	>500	>1000	n.d.	86.3	105.8	n.d.	69.7	85.6	n.d.
Mel M13	>500	496.0	>1000	62.3	1.6	11.5	67.8	3.2	10.5
Mel M14	>500	>1000	n.d.	56.3	26.3	n.d.	65.5	22.4	n.d.
Colo1	389.0	689.3	n.d.	10.2	49.8	n.d.	15.4	22.6	n.d.
Colo2	411.5	>1000	n.d.	18.6	50.5	n.d.	19.3	35.2	n.d.
BRCAN1	486.0	960.4	n.d.	12.6	6.5	n.d.	11.2	3.6	n.d.
BRCAN2	>500	>1000	n.d.	89.7	22.1	n.d.	67.2	19.5	n.d.
OVCA1	>500	>1000	n.d.	77.3	21.5	n.d.	71.5	16.3	n.d.
OVCA2	400.7	850.5	n.d.	22.7	11.5	n.d.	21.0	8.8	n.d.

*Dose–response curves for IC_{50} calculation were obtained by treating human tumor cells with CPL alone (highest dose = 500 μM), 5-FU alone (highest dose = 1 mg/mL) or VBL alone (highest dose = 1 μg/mL) or by pretreating them with omeprazole or esomeprazole for 24 hours before beginning the anticancer drug treatment. >500 μM for CPL, >1000 μg/mL for 5-FU, and 1000 ng/mL for VBL refer to the inability of the various cell lines to reach an IC_{50} value within the dose–response curve high limit in the absence of proton pump inhibitor pretreatment. IC_{50} = concentration that causes 50% cell death; n.d. = not determined; Mel = melanoma, Colo = colon adenocarcinoma, BRCAN = breast cancer, OVCA = ovarian adenocarcinoma.

Consistent with our hypothesis that omeprazole and antitumor drugs (e.g., cisplatin) would compete for cellular uptake and localization, thus weakening or inhibiting the effects of PPIs, omeprazole did not induce any change in the responsiveness of the same melanoma cells to cisplatin when administered simultaneously with the anticancer drug (Fig. 1, E).

To verify that PPIs could induce effectiveness of different classes of antitumor drugs, we tested the efficacy of omeprazole on tumor cell resistance to 5-FU, using cell lines resistant to this drug (Table 1). Dose–response curves were obtained from tumor cell lines of different histologies that had not been pretreated with omeprazole or that had been pretreated with this PPI for 24 hours and were then treated with five logarithmic dilutions of 5-FU (Fig. 2). Omeprazole pretreatment induced susceptibility to the cytotoxic effect of 5-FU in all the tumor cell lines tested, including two melanoma lines (Fig. 2, A and B) and one colon carcinoma line (Fig. 2, C). Again, simultaneous treatment with the PPI and 5-FU was ineffective (data not shown).

Using the same experimental protocol, we obtained dose–response curves of the effects of five logarithmic dilutions of vinblastine on tumor cell lines pretreated with omeprazole. Again, omeprazole pretreatment of melanoma cell lines intrinsically resistant to vinblastine (Table 1) resulted in their becoming sensitive to the cytotoxic effects of this drug (Fig. 3, A). Similar results were obtained with other PPIs (i.e., esomeprazole and pantoprazole) and other tumor cell lines (Table 1).

We also tested the effect of PPI pretreatment in cells that had been selected *in vitro* for a multidrug-resistant phenotype. For this analysis, we used CEM-VBL100 cells, which were obtained by selection of the parental human T-lymphoblastoid cell line CEM in a medium containing increasing concentrations of vinblastine *(34).* The results clearly showed that vinblastine sensitivity was restored in CEM-VBL100 cells after pretreating them with omeprazole (Fig. 3, B). Similar results were obtained with esomeprazole and pantoprazole (not shown). Again, omeprazole was ineffective when administered at the same time as vinblastine (data not shown). Interestingly, omeprazole was able to lower the minimal cytotoxic dose of vinblastine on the CEM drug-sensitive parental line (Fig. 3, C). Thus, PPI pretreatment not only induced susceptibility to anticancer drugs in tumor cells intrinsically resistant to such drugs but also reversed acquired multidrug resistance and increased cytotoxicity of antitumor treatments in drug-sensitive human tumor cells.

Effects of Omeprazole Treatment on Human Tumor Cell Lines

We next investigated how PPIs interfered with cellular functions that otherwise prevent cytotoxic drugs from exerting their cytotoxic effects. Thus, we analyzed the effects of 24 hours of PPI (omeprazole or esomeprazole) treatment on two human melanoma cell lines (MelP6 and MelM6). PPI treatment had no effect on cell viability or cell cycle progression (Fig. 4, A). We next compared the pH of the medium of PPI-treated and untreated human tumor cells. The results demonstrated that omeprazole impaired the ability of tumor cells to acidify the extra-

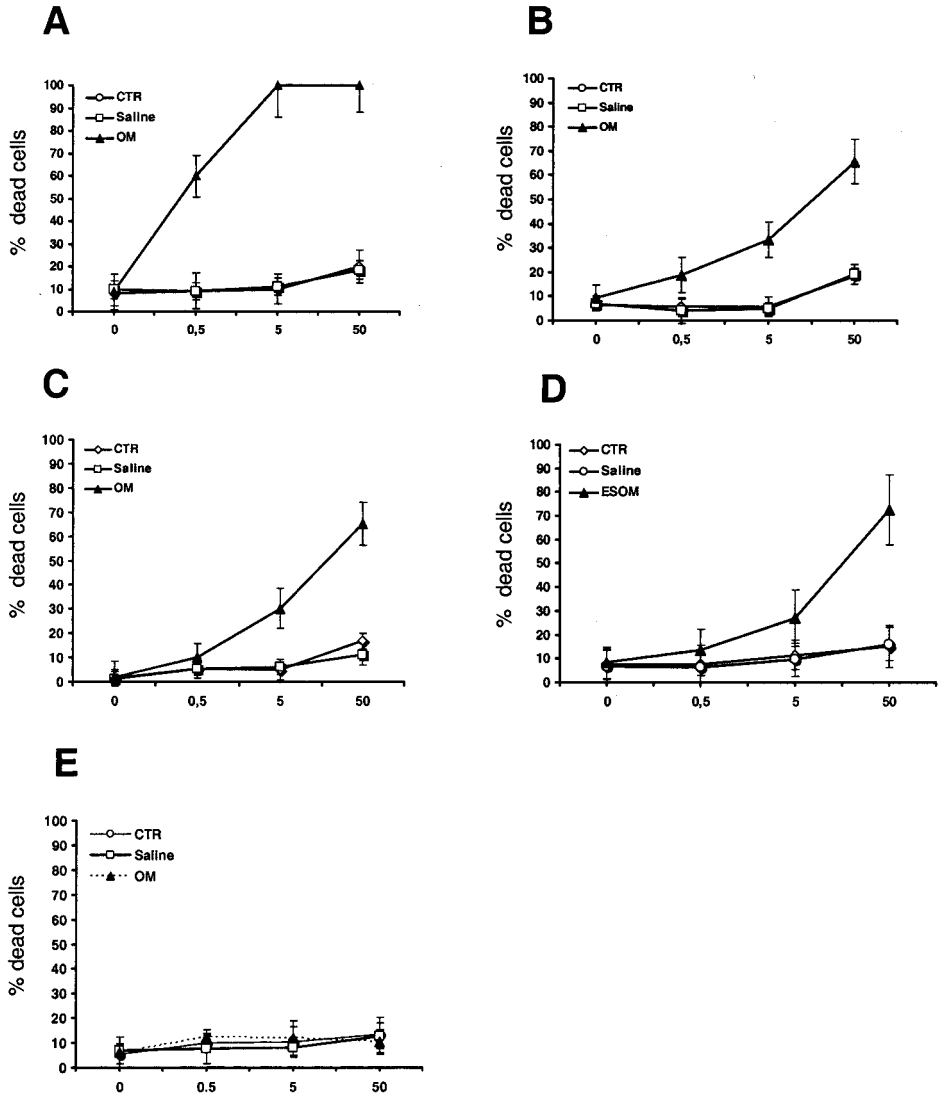

Fig. 1. Dose–response curves of cisplatin effects on cisplatin-resistant melanoma cell lines pretreated with proton pump inhibitors (PPIs). Cells were pretreated with a PPI or were not pretreated and were then treated with three log dilutions of cisplatin. **A**–**C**) Dose–response curves obtained by treating three human melanoma cell lines (MelP6, MelM6, MelM9) with cisplatin alone (CTR) or pretreating them with omeprazole (OM) or saline 24 hours before cisplatin treatment. **D**) Dose–response curve obtained by treating a human melanoma cell line (MelM6) with cisplatin alone (CTR) or with cisplatin after a 24-hour pretreatment with esomeprazole (ESOM) or saline. **E**) Dose–response curve obtained by treating human melanoma cells (MelM6) with cisplatin alone (CTR) or with cisplatin plus omeprazole (OM) or (saline). Cell death was assayed by using the trypan blue exclusion assay, and the results were verified with the LIVE/DEAD Viability/Cytotoxicity kit. The histograms represent mean ± 95% confidence intervals of five different experiments.

cellular medium as early as 3 hours after treatment (Fig. 4, B). Omeprazole treatment also induced an increase in lysosomal pH (Fig. 4, C). Moreover, LSCM analysis showed that the LysoSensor-positive acidic vesicles lost their secretory behavior and accumulated within the cell cytoplasm (Fig. 4, D).

Given the inhibitory effect of PPIs on V-H^+-ATPase activity in other cellular systems *(31–33),* we also analyzed both the expression and activity of V-H^+-ATPases in four human tumor cell lines (MelM1, MelM6, MelM9, MelP6) treated with omeprazole. Treatment with different doses of omeprazole did not induce a change in V-H^+-ATPase protein levels (Fig. 5, A). However, the subcellular localization changed, with V-H^+-ATPase–expressing vesicle-like structures accumulating in perinuclear regions of the omeprazole-treated cells (Fig. 5, B, lower panel). In fact, in untreated cells, V-H^+-ATPase staining appeared widely diffuse in the cytoplasm and beneath the cell membrane (Fig. 5, B, upper panel). This change in localization was accompanied by a change in levels of intracellular ATP. In fact, cells treated with omeprazole or esomeprazole had higher levels of intracellular ATP than untreated cells, suggesting potent inhibition of the V-H^+-ATPase activity (Fig. 5, C).

PPI Effect on Drug Efflux

We next investigated possible mechanisms responsible for the effect of PPI on tumor cell resistance to antitumor drugs. We used LSCM to monitor the intracellular distribution of fluorescently labeled (vinblastine-bodipy) or spontaneously fluorescent (doxorubicin) antitumor drugs in untreated or omeprazole-pretreated tumor cells in both the uptake and efflux phases. We first evaluated the effect of omeprazole on vinblastine-bodipy accumulation. Cells pretreated with omeprazole displayed a marked vinblastine accumulation in cytoplasmic vesicles 6 hours after the vinblastine-bodipy was added (Fig. 6, B), whereas cells that had not been pretreated displayed fluorescence diffused throughout the cytoplasm and in vesicle-like formations (Fig. 6, A). When cells were transferred to drug-free medium to allow drug efflux, cells that had been pretreated with omeprazole retained vinblastine-bodipy in vesicle-like structures (Fig. 6, D), whereas most vinblastine-bodipy was lost from cells that had not been pretreated (Fig. 6, C). The amount of retained antitumor drug was evaluated with LSCM. This analysis showed that, at the end of the uptake phase, the difference in mean pixel inten-

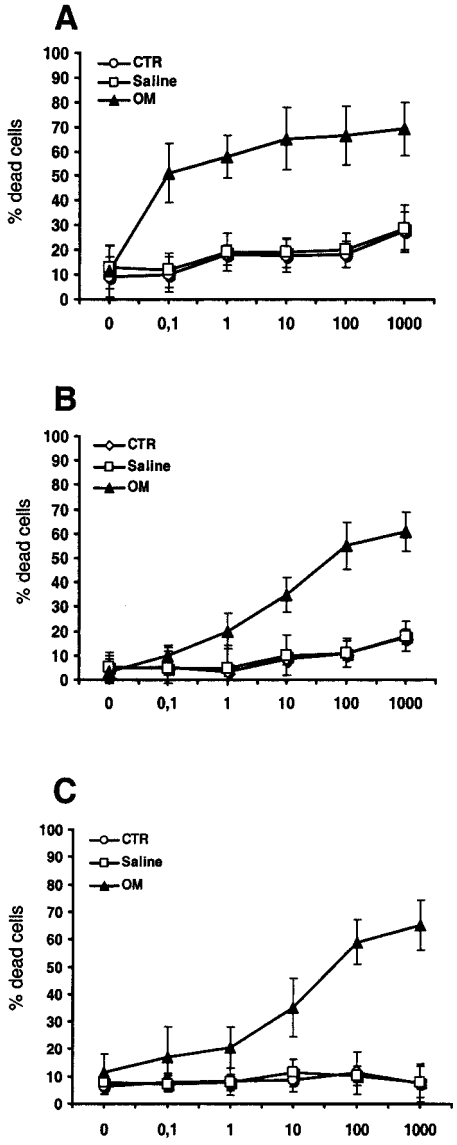

Fig. 2. Effects of omeprazole (OM) on 5-fluorouracil (5-FU) resistance. Dose–response curves were obtained from human melanoma (MelM6, MelP6) (**A, B**) or colon adenocarcinoma (Colo1) (**C**) cells treated with five logarithmic dilutions (*x*-axes, μg/mL) of 5-FU alone (CTR) or after a 24-hour pretreatment with OM. As a control (saline), cells were treated with 5-FU plus saline, saline being the medium in which omeprazole was solubilized. Cell death was assayed by using a trypan blue exclusion assay, and the results were verified with the LIVE/DEAD viability/Cytotoxicity kit. The histograms represent mean ± 95% confidence intervals of five different experiments.

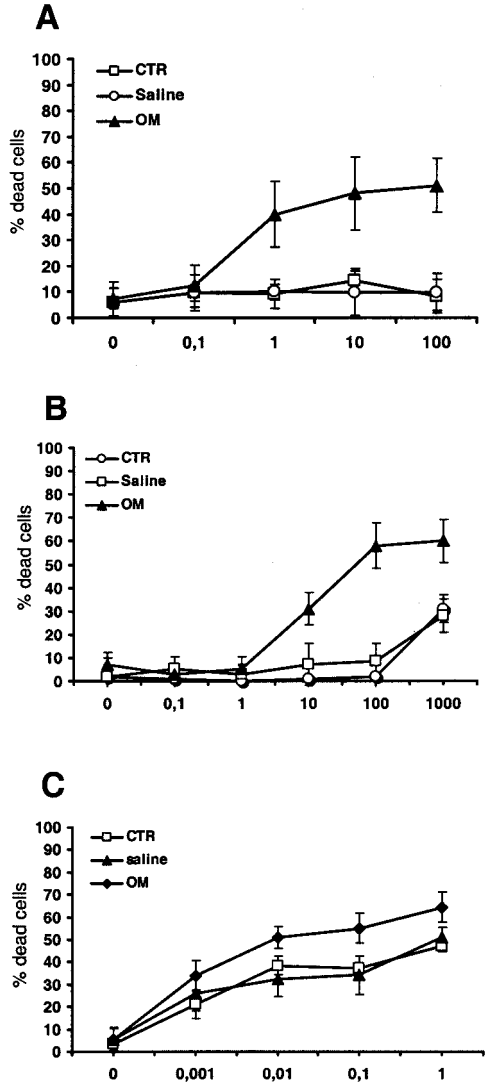

Fig. 3. Effects of omeprazole (OM) on vinblastine resistance, either intrinsic or induced. Dose–response curves were obtained by treating a melanoma cell line (MelM6; **panel A**), CEM-VBL100 (**panel B**), or CEM (**panel C**) with vinblastine alone (CTR) or after a 24-hour pretreatment with OM; experiments were performed in triplicate. As a control (saline), cells were pretreated with saline 24 hours before vinblastine administration. Cell death was assayed by using a trypan blue exclusion assay, and the results were verified with the LIVE/DEAD Viability/Cytotoxicity kit. The histograms represent mean ± 95% confidence intervals of five different experiments.

sities between cells that were pretreated with omeprazole (45.78) and cells that were not pretreated (48.84) was not statistically significant (3.06, 95% CI = −3.46 to 9.58; P = .55). However, at the end of the efflux phase, the difference in mean pixel intensities of the retained fluorescent drug between tumor cells pretreated with omeprazole (52.71) and cells not treated with omeprazole (20.09) was statistically significant (32.62, 95% CI = 23.08 to 42.16; $P<.001$). These results suggest that omeprazole pretreatment does not influence the uptake phase of the antitumor drug but strongly inhibits the elimination of antitumor drugs through the secretory pathway.

We next investigated the localization of a nuclear-targeted antitumor drug (i.e., doxorubicin) (Fig. 6, E–L). Whereas omeprazole pretreatment only slightly increased doxorubicin uptake in tumor cells as compared with untreated cells (Fig. 6, E and F), doxorubicin was completely retained in omeprazole-pretreated cells within vesicle-like structures, even after 24 hours in drug-free medium (Fig. 6, G and H). By 36 hours, doxorubicin was detectable in the nuclei of PPI-treated cells (Fig. 6, I and L). Thus, PPI treatment induced a massive retention of doxorubicin within vesicle-like structures, allowing this drug to get to the nucleus.

Effects of Omeprazole on Sensitivity of Human Tumors to Antitumor Agents in SCID Mice Engrafted With Human Tumor Cells

To assess the potential clinical relevance of the *in vitro* results, we performed *in vivo* experiments in a human/mouse

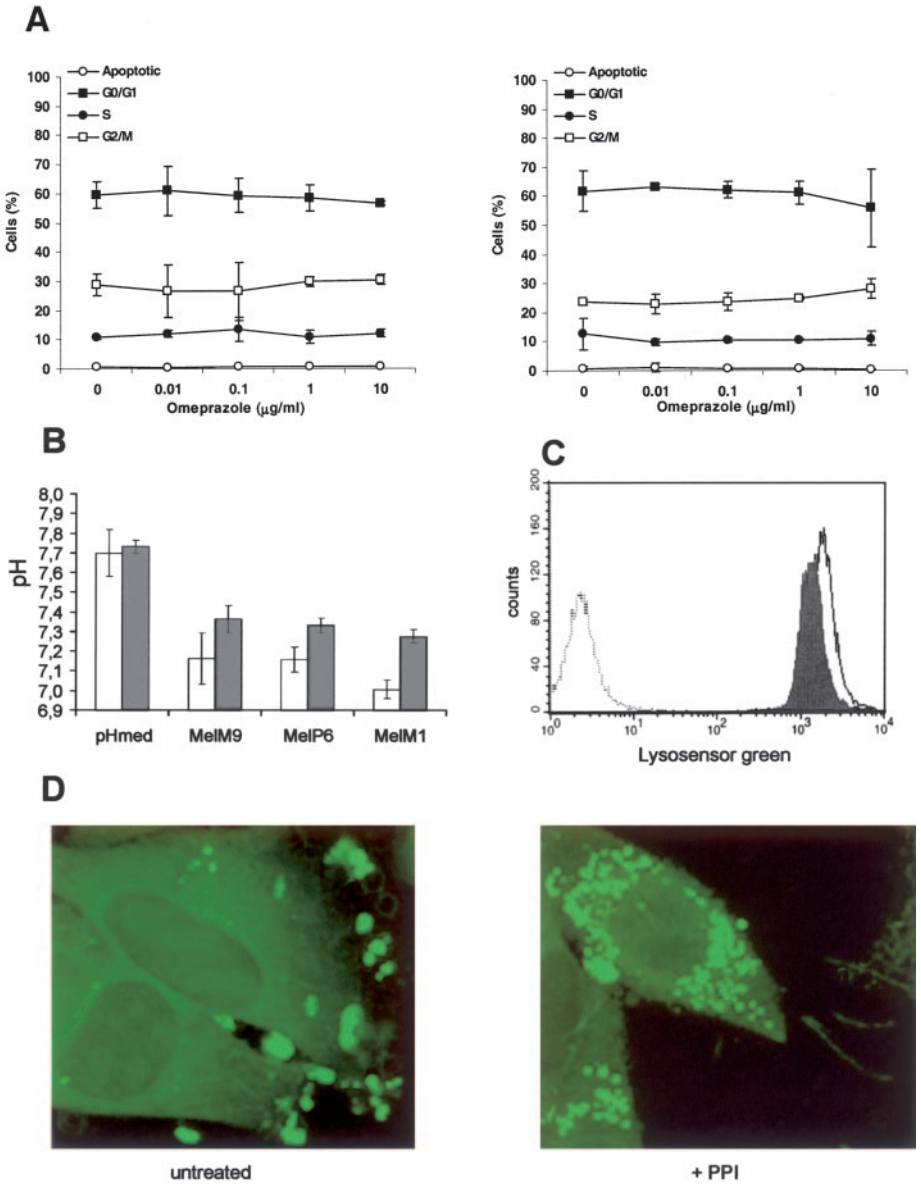

Fig. 4. Effects of omeprazole on cell cycle and cellular pH. **A**) Effects of omeprazole on cell cycle and apoptosis of MelM6 (**right panel**) and MelP6 (**left panel**) human melanoma cells after a 24-hour treatment. **B**) Histograms represent mean value ± 95% confidence intervals of at least three extracellular medium pH determinations on three melanoma cell lines untreated (**white bar**) or treated with omeprazole (**gray bar**). **C**) The fluorescence intensity of human MelM6 melanoma cells stained with LysoSensor Green DND-189 probe. The **dotted line** shows the background fluorescence from untreated and unstained cells and the **black line** shows that from untreated cells stained with the probe. The **filled gray area** represents the fluorescence from cells treated with omeprazole and stained with the probe. **D**) The distribution of LysoSensor-positive acidic vesicles in MelM6 cells pretreated (**right**) with omeprazole or not pretreated (**left**).

model system represented by CB.17 SCID/SCID mice injected subcutaneously with human melanoma cells (MelM6). These mice have proved useful in assessing the *in vivo* efficacy of local and systemic antitumor treatments *(39,43–45).* Mice engrafted with human tumor cells were pretreated in groups of 10 with omeprazole administered orally (by gavage); 24 hours later, they were injected intraperitoneally with a single dose of cisplatin. Tumor growth was then followed three times per week. Figure 7, A, shows that tumors in mice pretreated with omeprazole and then treated with cisplatin grew more slowly (mean tumor weight 16 days after treatment = 2788 mg) than tumors in mice that were treated with cisplatin but had not been pretreated with omeprazole (mean tumor weight 16 days after treatment = 7373 mg) for a difference at 16 days after treatment of 4585 mg (95% CI = 3711 to 5459) (Fig. 7, A). Again, consistent with the *in vitro* results, simultaneous treatment with cisplatin and omeprazole of melanoma-bearing SCID mice *in vivo* did not have any statistically significant effect on tumor growth (mean tumor weight 16 days after treatment = 7749 mg; difference versus non-pretreated mice = 376 mg, 95% CI = −1062 to 1814) (Fig. 7, A) Similar results were obtained with esomeprazole (data not shown). Histologic examination of the human tumors after the animals were killed showed that, in the omeprazole–cisplatin-treated mice, the tumor mass was occupied by large necrotic areas that accounted for most of the tumor size (Fig. 7, B), suggesting that the cytotoxic effect was greater than that quantified by the *in vivo* tumor size measurements. Mice were followed for 1 month, and the tumors of mice pretreated with omeprazole slowly regained their growth but never reached the size of the tumors in non-pretreated mice or in mice treated with ineffective therapeutic regimens (i.e., normal saline; data not shown). Melanoma-bearing SCID mice treated with cisplatin after omeprazole pretreatment did not show any signs of systemic toxicity such as weight loss, diarrhea, or hair ruffling (data not shown).

Discussion

The major hypothesis of this study was that the intrinsic resistance of tumors to cytotoxic drugs could be inhibited by

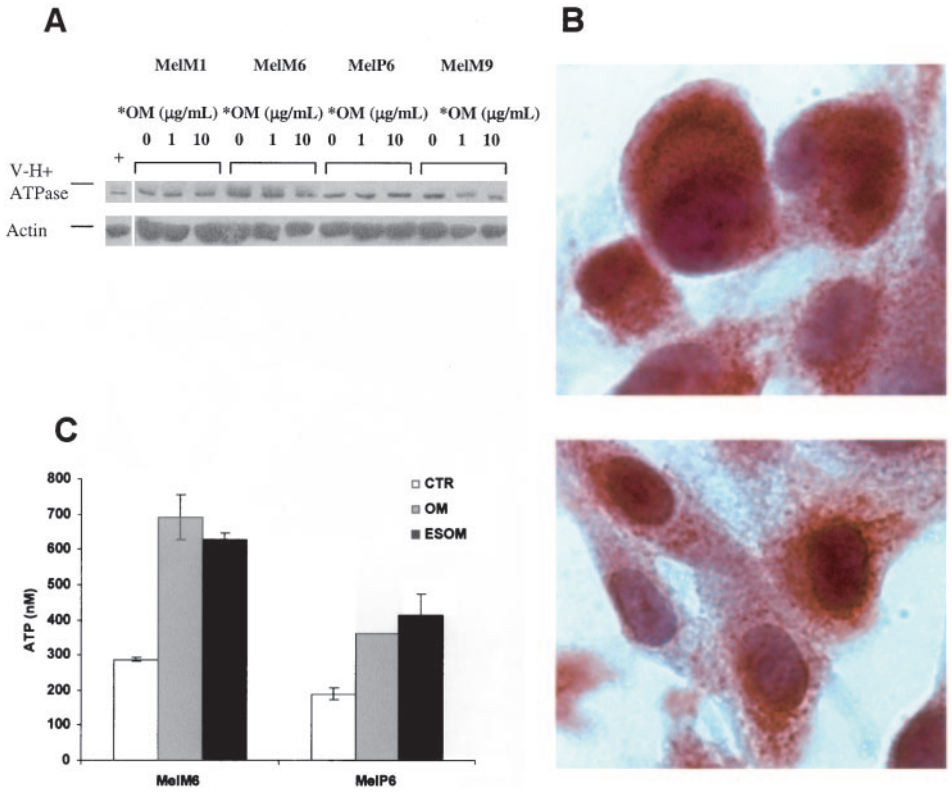

Fig. 5. Effects of proton pump inhibitors (PPIs) on V-H^+-ATPase activity and distribution. **A**) Western blotting analysis of V-H^+-ATPase protein expression in four human melanoma cell lines after 24-hour treatment with omeprazole (OM). HeLa cells (+) were used as positive control. **B**) The distribution of V-H^+-ATPase-expressing vesicles in PPI-treated (**lower panel**) or untreated (**upper panel**) melanoma cells. **C**) The effect of OM and esomeprazole (ESOM) treatment (1 μg/mL) on intracellular ATP in human melanoma cell lines.

agents that affect the function of proton pumps that regulate cellular pH gradients. This hypothesis was based on previous findings that a marked alteration of the intra- to extracellular pH gradient occurs in malignant tumors, such that the extracellular compartments become highly acidic *(4,5,46),* and the acidic microenvironment and acidic vesicles *(2,3,6,7,9)* exert a major role in tumor resistance to cytotoxic drugs. We studied PPIs because these drugs inhibit the activity of V-H^+-ATPases *(31–33),* which are known to be highly expressed in tumors *(5,19,46–48)* and activated exclusively in acidic sites. We found that pretreatment with PPIs consistently induced susceptibility of tumor cells of multiple histologies to the cytotoxic effect of different antitumor drugs, with a marked reduction of drug efflux; that the effect of PPI was mediated by an increase of both extracellular and intracellular pH and by an inhibition of V-H^+-ATPase activity; and that oral pretreatment of xenograft mouse models with omeprazole caused human solid tumors resistant to cisplatin to become sensitive to this drug. Taken together, these data suggest that pretreatment with PPIs may represent a powerful strategy for treating human solid tumors refractory to cytotoxic drugs. PPIs were also able to increase the effect of antitumor drugs in sensitive cells, suggesting that PPI pretreatment may be useful in increasing the efficacy of antitumor drugs even in drug-sensitive tumors.

We also found that simultaneous treatment with PPIs and the antitumor drugs was ineffective, both *in vitro* and *in vivo.* A possible explanation for this phenomenon may lie in the documented ability of some cytotoxic drugs, such as cisplatin, to increase the activity of V-H^+-ATPases in treated cells *(25).* It is also conceivable that the simultaneous administration of PPI and the weakly basic cytotoxic drug may lead to a competition between the two drugs for the tumor acidic environment. This competition may in turn lead, on one hand, to the inactivation of the cytotoxic drugs or, on the other hand, to the nonactivation of the PPI, which needs to be protonated to work.

Our results suggest that the induction of susceptibility to anticancer drugs following PPI pretreatment involves the inhibition of acidification of the tumor environment. In fact, our results showed that PPI treatment of tumor cells increases both the extracellular pH and the pH of lysosomal-like organelles, consistent with the inhibition of ATPase activity and without evidence of cytotoxicity. We also showed that PPI pretreatment inhibits the secretory behavior of the vesicular structures in which the antitumor drugs accumulate. Moreover, our finding that, 36 hours after doxorubicin treatment of PPI-pretreated cells, the drug had reached the nucleus suggests that drug retention in cytoplasmic vesicles following PPI pretreatment was a temporary phenomenon that did not lead to drug elimination or inactivation. In fact, in untreated tumor cells, acidic vesicles actively degranulated in the extracellular environment, and the cytotoxic drug (i.e., doxorubicin) accumulated in cytoplasmic vesicles only temporarily during the uptake period and was quickly eliminated during the observation period (i.e., in drug-free medium).

Thus, a quick elimination through acidic vesicles may be a key mechanism for tumor refractoriness to cytotoxic drugs, as suggested in previous studies *(6,7,9–12,17).* Our study provides evidence that tumor cells may make use of this quick elimination function to render antitumor drugs ineffective through one of two related mechanisms: 1) acidifying the extracellular environment and thereby neutralizing those antitumor drugs that are weak bases, or 2) sequestering drugs in acidic vesicles and/or eliminating them through an exocytotic pathway, a mechanism that would allow tumor cells to eliminate a wider spectrum of antitumor drugs. Tumor activities include phagocytosis of apoptotic material through acidic vacuoles *(38),* as well as the

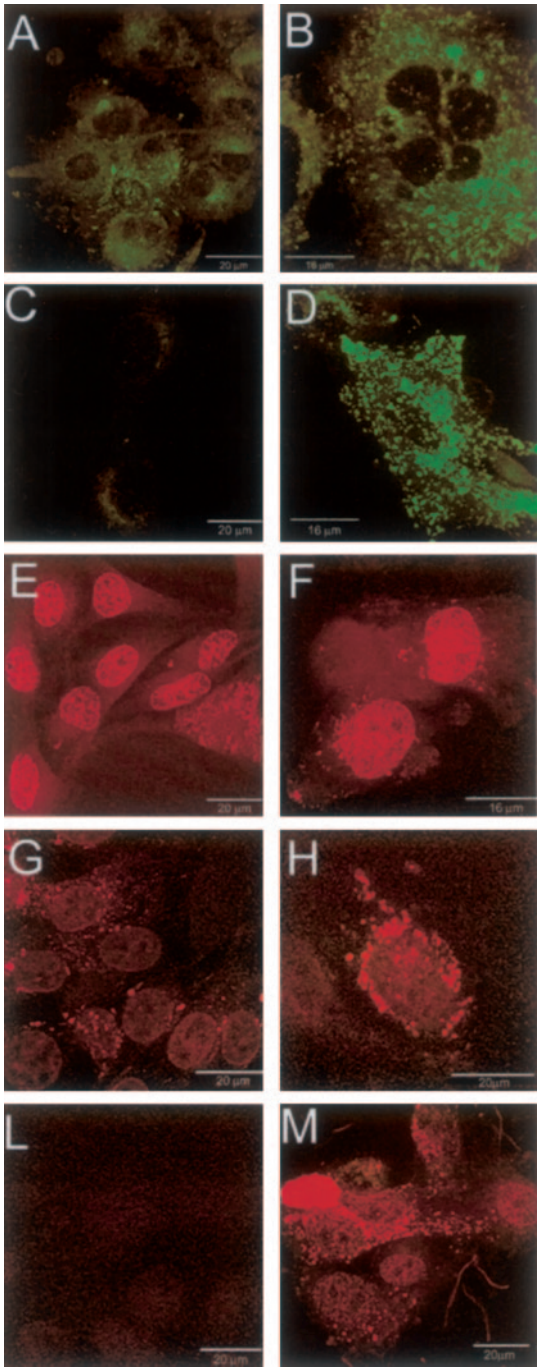

Fig. 6. Effects of omeprazole on drug efflux. A representative result of the laser scanning confocal analysis of a human melanoma cell line (MelM6) treated with fluorescent drugs alone (**left panels**) or after a 24-hour pretreatment with omeprazole (**right panels**) is shown. Uptake phase: **panels A**, **B**, **E**, and **F** show melanoma cells after a 6-hour incubation with vinblastine bodipy (**A** and **B**) or doxorubicin (**E** and **F**). Efflux phase: after 6 hours of drug uptake, cells were allowed to efflux in vinblastine-bodipy–free medium for 18 hours (**C** and **D**) or in doxorubicin-free medium for 18 (**G** and **H**) or 36 hours (**I** and **L**). Magnification = 750×.

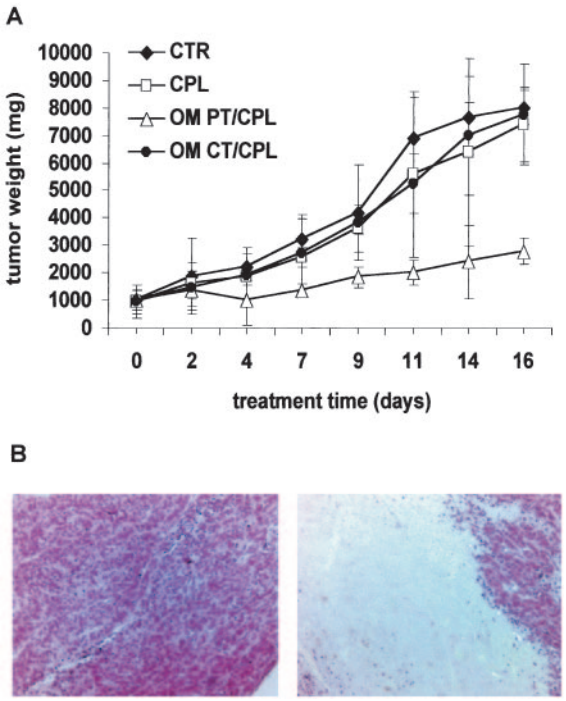

Fig. 7. *In vivo* effects of omeprazole on tumor growth in the human tumor/SCID mouse model. CB.17 SCID/SCID mice were engrafted with MelM9 melanoma cells via subcutaneous injection in the right flank. At the time of tumor appearance (approximately 7–10 days after injection), mice were left untreated or were treated with various combinations of omeprazole (a single gavage treatment) and cisplatin (a single intraperitoneal treatment). **A**) Mean results of three representative experiments (each experiment on at least 10 mice) on CB.17 SCID/SCID mice engrafted with a human melanoma cell line derived from a primary lesion. Mice were treated with cisplatin alone (CPL), with cisplatin 24 hours after omeprazole pretreatment (OM PT/CPL), with cisplatin and omeprazole at the same time (OM CT/CPL), or left untreated (CTR).Tumor size was measured three times per week with calipers, and volume was calculated as described in the "Methods" section. The histograms represent mean ± 95% confidence intervals of tumor weight. **B**) Representative tumors resected from a mouse treated with cisplatin alone (**left panel**) and a mouse pretreated with omeprazole (**right panel**). Tumors were stained with hematoxylin and eosin. In the omeprazole–cisplatin-treated tumor, the tumor mass was occupied by a large necrotic area that mostly accounted for the tumor size (magnification = 125×).

degranulation of microvesicles that are able to kill lymphocytes through apoptotic pathways *(49).* It is therefore conceivable that the traffic of acidic vacuoles and microvesicles may have a prominent role in tumor homeostasis.

Our findings add to the understanding of the resistance of human tumors to cytotoxic drugs in an additional way. We have shown here that human melanoma and adenocarcinoma cells express substantial levels of V-H^+-ATPases and that PPI treatment of tumor cells, while not affecting the level of V-H^+-ATPase protein, inhibits its activity and changes its subcellular localization. Thus, inhibition of V-H^+-ATPase activity may represent an important mechanism of action of PPIs in their effect on tumor drug resistance. In fact, V-H^+-ATPases carry out ATP-dependent proton transport from the cytoplasmic compartment to the opposite side of the membrane (the lumen of an intracellular vesicle or the extracellular space) *(19),* thus contributing to the creation and maintenance of the acidic microenvironment of tumors. Recent data suggest that V-H^+-ATPase may be anchored, via its subunit C or ezrin adaptor protein, to the actin cytoskeleton *(50,51).* We have recently shown that ezrin, radixin, and moesin may exert an important role in multidrug resistance by mediating the P-glycoprotein linkage to actin *(36);* indeed, the function of a growing number of efflux pumps seems to depend on their connection to the cytoskeleton *(52).* Moreover, the ezrin and actin connection seems to have an important role in the trafficking of

acidic vesicles in human malignant tumors *(38).* It is therefore conceivable that connection to the cytoskeleton may have a key role for V-H^+-ATPase activity as well. This, in turn, suggests that combined strategies aimed at inhibiting tumor acidity or at inhibiting connections between actin and the ion pumps may be extremely effective in depriving tumors of drug resistance strategies.

An important finding from our study is that PPI pretreatment predisposes melanoma and adenocarcinoma cells to the effects of different classes of antitumor agents, including cisplatin, whose mechanism of resistance is poorly known; 5-FU, whose main resistance mechanism is thought to be based on gene mutation *(53);* and vinblastine, a specific substrate of resistance-conferring proteins such as P-glycoprotein *(12).* Hence, our results suggest that PPIs are potentially powerful tools in the treatment of human solid tumors because they may induce sensitivity to a wide range of antitumor drugs. There is already a considerable record of the clinical use of PPIs as anti-acid drugs in the treatment of peptic diseases without any described toxic effect on patients. It is therefore conceivable that this class of drugs can be rapidly tested for efficacy in preventing or reversing resistance to antitumor drugs in cancer patients.

REFERENCES

(1) Gottesman MM, Pastan I. Biochemistry of multidrug resistance mediated by the multidrug transporter. Annu Rev Biochem 1993;62:385–427.

(2) Mahoney BP, Raghunand N, Bagget B, Gillies RJ. Tumor acidity, ion trapping and chemotherapeutics I. Acid pH affects the distribution of chemotherapeutic agents in vitro. Biochem Pharmacol 2003;66:1207–18.

(3) Simon S, Roy D, Schindler M. Intracellular pH and the control of multidrug resistance. Proc Natl Acad Sci U S A 1994;91:1128–32.

(4) Tannock IF, Rotin D. Acid pH in tumors and its potential for therapeutic exploitation. Cancer Res 1989;49:4373–84.

(5) Izumi H, Torigoe T, Ishiguchu H, Uramoto H, Yoshida Y, Tanabe M, et al. Cellular pH regulators: potentially promising molecular targets for cancer chemotherapy. Cancer Treat Rev 2003;29:541–9.

(6) Raghunand N, He X, van Sluis R, Mahoney BP, Bagget B, Tayloe CW, et al. Enhancement of chemotherapy by manipulation of tumor pH. Br J Cancer 1999;80:1005–11.

(7) Raghunand N, Martinez-Zaguilan R, Wright SH, Gillies RJ. pH and drug resistance. II. Turnover of acidic vesicles and resistance to weakly basic chemotherapeutic drugs. Biochem Pharmacol 1999;57:1047–58.

(8) Raghunand N, Mahoney BP, Gillies RJ. Tumor acidity, ion trapping and chemotherapeutics II. pH-dependent partition coefficients predict importance of ion trapping on pharmacokinetics of weakly basic therapeutic agents. Biochem Pharmacol 2003;66:1219–29.

(9) Altan N, Chen Y, Schindler M, Sanford SM. Defective acidification in human breast tumor cells and implications for chemotherapy. J Exp Med 1998;187:1583–98.

(10) Hurwitz SJ, Terashima M, Mizunuma N, Slapak CA. Vesicular anthracycline accumulation in doxorubicin-selected U937 cells: participation of lysosomes. Blood 1997;89:3745–54.

(11) Schindler M, Grabski S, Hoff E, Simon SM. Defective pH regulation of acidic compartments in human breast cancer cells (MCF-7) is normalized in adriamycin-resistant cells (MCF-7adr). Biochemistry 1996;35:2811–7.

(12) Larsen AK, Escargueil AE, Skladanowski A. Resistance mechanisms associated with altered intracellular distribution of anticancer agents. Pharmacol Ther 2000;85:217–29.

(13) Bour-Dill C, Gramain MP, Merlin JL, Marchal S, Guillemin F. Determination of intracellular organelles implicated in daunorubicin cytoplasmic sequestration in multidrug-resistant MCF-7 cells using fluorescence microscopy image analysis. Cytometry 2000;39:16–25.

(14) Cleary I, Doherty G, Moran E, Clynes M. The multidrug-resistant human lung tumour cell line, DLKP-A10, expresses novel drug accumulation and sequestration systems. Biochem Pharmacol 1997;53:1493–502.

(15) Bobichon H, Colin M, Depierreux C, Liautaud-Roger F, Jardillier JC. Ultrastructural changes related to multidrug resistance in CEM cells: role of cytoplasmic vesicles in drug exclusion. J Exp Ther Oncol 1996;1:49–61.

(16) Dietel M, Arps H, Lage H, Niendorf A. Membrane vesicle formation due to acquired mitoxantrone resistance in human gastric carcinoma cell line EPG85-257. Cancer Res 1990;50:6100–6.

(17) Ouar Z, Lacave R, Bens M, Vandewalle A. Mechanisms of altered sequestration and efflux of chemotherapeutic drugs by multidrug resistant cells. Cell Biol Toxicol 1999;15:91–100.

(18) Ouar Z, Bens M, Vignes C, Paulais M, Pringel C, Fleury J, et al. Inhibitors of vacuolar H+-ATPase impair the preferential accumulation of daunomycin in lysosomes and reverse the resistance to anthracyclines in drug-resistant renal epithelial cells. Biochem J 2003;370:185–93.

(19) Nishi T, Forgac M. The vacuolar (H+)-ATPases—nature's most versatile proton pumps. Nat Rev Mol Cell Biol 2002;3:94–103.

(20) Beck WT. The cell biology of multiple drug resistance. Biochem Pharmacol 1987;36:2879–87.

(21) Vaananen HK, Karhukorpi EK, Sunquist K, Wallmark B, Roinine I, Hentune T, et al. Evidence of the presence of H+-ATPase types in the ruffled borders of osteoclasts. J Cell Biol 1990;111:1305–11.

(22) Marquardt D, Center MS. Involvement of vacuolar H+-adenosine triphosphatase activity in multidrug resistance in HL60 cells. J Natl Cancer Inst 1991;83:1098–1102.

(23) Martinez-Zaguilan R, Lynch RM, Martinez GM, Gillies RJ. Vacuolar-type H(+)-ATPases are functionally expressed in the plasma membranes of human tumor cells. Am J Physiol 1993;265(4 Pt 1):C1015–29.

(24) Moriyama Y. Membrane energization by proton pumps is important for compartmentalization of drugs and toxins: a new type of active transport. J Exp Biol 1996;199:1447–54.

(25) Murakami T, Shibuya I, Ise T, Chen ZS, Akiyama S, Nakagawa M, et al. Elevated expression of vacuolar proton pump genes and cellular pH in cisplatin resistance. Int J Cancer 2001;93:869–74.

(26) Horn J. The proton-pump inhibitors: similarities and differences. Clin Ther 2000;22:266–80.

(27) Wallmark B, Larsson H, Humble L. The relationship between gastric acid secretion and gastric H+, K+-ATPase activity. J Biol Chem 1985;260:13681–4.

(28) Wallmark B, Lorentzon P, Larsson H. The mechanism of action of omeprazole—a survey of its inhibitory action in vitro. Scand J Gastroenterol Suppl 1985;108:37–51.

(29) Puscas I, Coltau M, Baican M, Domuta G. Omeprazole has a dual mechanism of action: it inhibits both H(+)K(+)ATPase and gastric mucosa carbonic anhydrase enzyme in humans (in vitro and in vivo experiments). J Pharmacol Exp Ther 1999;290:530–4.

(30) Larsson H, Mattson H, Sundell G, Carlsson E. Animal pharmacodynamics of omeprazole. A survey of its pharmacological properties in vivo. Scand J Gastroenterol Suppl 1985;108:23–35.

(31) Mizunashi K, Furukawa Y, Katano K, Abe K. Effect of omeprazole, an inhibitor of H+,K(+)-ATPase, on bone resorption in humans. Calcif Tissue Int 1993;53:21–5.

(32) Graber ML, Devine P. Omeprazole and SCH 28080 inhibit acid secretion by the turtle urinary bladder. Ren Physiol Biochem 1993;16:257–67.

(33) Sabolic I, Brown D, Verbavatz JM, Kleinman J. H(+)-ATPases of renal cortical and medullary endosomes are differentially sensitive to Sch-28080 and omeprazole. Am J Physiol 1994;266(6 Pt 2):F868–77.

(34) Cianfriglia M, Cenciarelli C, Tombesi M, Barca S, Mariani M, Morroni S, et al. Murine monoclonal antibody recognizing a 90-kDa cell-surface determinant selectively lost by multi-drug-resistant variants of CEM cells. Int J Cancer 1990;45:95–103.

(35) Luciani F, Matarrese P, Giammarioli AM, Lugini L, Lozupone F, Federici C, et al. CD95/phosphorylated ezrin association underlies HIV-1 GP120/IL-2-induced susceptibility to CD95 (APO-1/Fas)-mediated apoptosis of human resting CD4(+)T lymphoctes. Cell Death Differ 2004;11:574–82.

(36) Luciani F, Molinari A, Lozupone F, Calcabrini A, Lugini L, Stringaro A, et al. P-glycoprotein/actin association through ERM family proteins: a role in P-glycoprotein function in human cells of lymphoid origin. Blood 2002;99:641–8.

(37) Garewal HS, Ahmann FR, Schifman RB, Celniker A. ATP assay: ability to distinguish cytostatic from cytocidal anticancer drug effects. J Natl Cancer Inst 1986;77:1039–45.

(38) Lugini L, Lozupone F, Matarrese P, Funaro C, Luciani F, Malorni W, et al. Potent phagocytic activity discriminates metastatic and primary human malignant melanomas: a key role of ezrin. Lab Investig 2003;83:1555–67.
(39) Bosma MJ, Carroll AM. The SCID mouse mutant: definition, characterization, and potential uses. Annu Rev Immunol 1991;9:323–50.
(40) Watson SA, Smith AM. Hypergastrinaemia promotes adenomaprogression in the APCMin7/+ mouse model of familial adenomatous polyposis. Cancer Res 2001;61:625–31.
(41) Son K, Huang L. Exposure of human ovarian carcinoma to cisplatin transiently sensitizes the tumor cells for liposome-mediated gene transfer. Proc Natl Acad Sci U S A 1994;91:12669–72.
(42) Geran RI, Greenberg NH, Macdonald MM, Shumacher AM, Abbot BJ. Protocols for screening chemical agents and natural products against animal tumors and natural other biological systems. Cancer Chemother Rep 1972;3:1–88.
(43) Lozupone F, Luciani F, Venditti M, Rivoltini L, Pupa S, Parmiani G, et al. Murine granulocytes control human tumor growth in SCID mice. Int J Cancer 2000;87:569–73.
(44) Lozupone F, Rivoltini L, Luciani F, Venditti M, Lugini L, Cova A, et al. Adoptive transfer of an anti-MART-1(27-35)-specific CD8+ T cell clone leads to immunoselection of human melanoma antigen-loss variants in SCID mice. Eur J Immunol 2003;33:556–66.
(45) Lozupone F, Pende D, Burgio VL, Castelli C, Spada M, Venditti M, et al. Effect of human natural killer and gammadelta T cells on the growth of human autologous melanoma xenografts in SCID mice. Cancer Res 2004;64:378–85.
(46) Martinez-Zaguilan R, Raghunand N, Lynch RM, Bellamy W, Martinez GM, Rojas B, et al. pH and drug resistance. I. Functional expression of plasmalemmal V-type H+-ATPase in drug-resistant human breast carcinoma cell lines. Biochem Pharmacol 1999;57:1037–46.
(47) Sennoune SR, Bakunts K, Martinez GM, Chua-Tuan JL, Kebir Y, Attaya MN, et al. Vacuolar H+-ATPase in human breast cancer cells with distinct metastatic potential: distribution and functional activity. Am J Physiol Cell Physiol 2004;286:C1443–52.
(48) Torigoe T, Izumi H, Murakami T, Uramoto H, Ishiguchi H, Yoshida Y, et al. Vacuolar H(+)-ATPase: functional mechanisms and potential as a target for cancer chemotherapy. Anticancer Drugs 2002;13:237–43.
(49) Andreola G, Rivoltini L, Castelli C, Huber V, Perego P, Deho P, et al. Induction of lymphocyte apoptosis by tumor cell secretion of FasL-bearing microvesicles. J Exp Med 2002;195:1303–16.
(50) Vitavska O, Wieczorek H, Merzendorfer H. A novel role for subunit C in mediating binding of the H+-V-ATPase to the actin cytoskeleton. J Biol Chem 2003;278:18499–505.
(51) Zhou R, Cao X, Watson C, Miao Y, Guo Z, Forte JG, et al. Characterization of protein kinase A-mediated phosphorylation of ezrin in gastric parietal cell activation. J Biol Chem 2003;278:35651–9.
(52) Chasan B, Geisse NA, Pedatella K, Wooster DG, Teintze M, Carattino MD, et al. Evidence for direct interaction between actin and the cystic fibrosis transmembrane conductance regulator. Eur Biophys J 2002;30:617–24.
(53) Longley DB, Harkin DP, Johnston PG. 5-Fluorouracil: mechanisms of action and clinical strategies. Nat Rev Cancer 2003;3:330–8.

NOTES

Supported by a grant from the Italian Ministry of Health. F. Luciani and L. Lugini were supported by a fellowship from Fondazione Italiana per la Ricerca sul Cancro (F.I.R.C.). A. De Milito was supported by a grant from the Swedish Research Council.

Manuscript received March 24, 2004; revised August 12, 2004; accepted September 7, 2004.